THE UNIVERSITY OF MICHIGAN

COLLEGE OF ENGINEERING

Department of Aerospace Engineering

High Altitude Engineering Laboratory

Scientific Report

# NEUTRAL COMPOSITION

E. J. Schaefer

ORA Project 05627

under contract with:

NATIONAL AERONAUTICS AND SPACE ADMINISTRATION
CONTRACT NO. NASr-54(05)
WASHINGTON, D. C.

administered through:

OFFICE OF RESEARCH ADMINISTRATION ANN ARBOR

February 1966

# NEUTRAL COMPOSITION

E. J. Schaefer

(Presented at the Second Conference on Direct Aeronomic Measurements in the Lower Ionosphere, University of Illinois, September 27-30, 1965)

## 1. Introduction

The incomplete knowledge of the composition of our atmosphere is due to the complexity of the problem and the inherent difficulties in conducting sufficiently precise measurement. Considerable effort has been focused on these problems in recent years and results are now beginning to emerge. The difficulties inherent in measuring the composition will be outlined and some techniques employed to overcome these difficulties will be described. Finally, some recent results illustrating diurnal and latitude variations in the composition of the upper atmosphere will be presented.

## 2. Ion Sources

A neutral particle mass spectrometer first ionizes a sample of the gas and then analyzes the ions in accordance with their charge-mass ratio. Establishing the relationship between the analyzed stream of ions and the ambient neutral composition is probably the greatest single source of error in the measurements. The two major uncertainties with which the experimenter must contend are recombination of reactive species, notably atomic oxygen (O), on the surfaces of the ion source and the dynamic effects arising from the vehicle velocity.

2.1 Recombination

Experimental determinations of the probability of recombination of O upon collision with platinum and aluminum surfaces have been reported to be of the order of one per cent per collision.[1,2] With this probability, only 36% of the original O would remain after 100 collisions and less than 0.01% after 1000 collisions. This is undoubtedly the reason for the low values of O obtained with the Bennett tube by Meadows and Townsend[3] and by Pokhunkov.[4-7] If very many collisions are involved, corrections for recombination effects are subject to large errors due to the large effect a small change in the assumed recombination probability will have on the fraction of O remaining for analysis.

Several methods to eliminate or circumvent this problem have been employed. The principle of most of these is to reduce the number of surface collisions prior to ionization and analysis to a minimum. Fig. 1 illustrates an open ion source employed by the University of Michigan. In operation, this source is immersed directly in the ambient atmosphere, thereby reducing the number of collisions to the order of one or two prior to ionization. Hence recombination effects are small. This ion source was the first to yield a reasonable measurement of the ambient O. The same principle has been employed by Nier et al[8,9] using a magnetic mass spectrometer. Fig. 2 illustrates the arrangment of three mass spectrometers and their ion sources flown recently by Nier. One ion source is open while two were flown in a cavity.

The dramatic difference in the O observed by the cavity and open instruments which were otherwise similar is conclusive evidence of the need to minimize surface collisions. (The second cavity instrument continuously monitered $N_2$.) Another open ion source which was used on Explorer XVII is described by Spencer and Reber.[10] Ionization of the gas was performed outside the satellite skin to avoid surface collision. An interesting alternate approach employed by the Southwest Center for Advanced Studies is illustrated in Fig. 3. Here the ion source is directed into the velocity vector. A small retarding potential in the ionization region rejects all ions except those possessing an energy equivalent to the vehicle velocity. Thus only those ions formed directly from the incoming stream of molecules are admitted to the analyzer. Unfortunately, satellite velocities are required to provide a practical stream input energy to serve as a basis for discrimination. Hence this technique does not appear applicable to sounding rockets.

2.2 Dynamic effects

The relation of the number density of a given stable species of gas in a moving orificed cavity to the ambient number density has been derived by Horowitz and LaGow[11]

$$n_a = n_g \sqrt{\frac{T_g}{T_a}} \Big/ \left[ e^{-s^2} + s\sqrt{\pi}\,(1 + \operatorname{erf} s) \right] \quad (1)$$

where $n_a$ = ambient number density

$n_g$ = number density of particles in gage

$T_a$ = ambient temperature

$T_g$ = gage temperature

$s$ = speed ratio = $V \Big/ \sqrt{\frac{2kT_a}{m}}$

$V$ = velocity of orifice normal to opening

$k$ = Boltzmann's constant = $1.38 \times 10^{-16}$ Erg $Deg^{-1}$ K

$m$ = particle mass in grams

Here several collisions with the cavity wall prior to ionization or escape are postulated thus permitting one to assume complete thermal accommodation of the gas within the cavity. Unfortunately, resorting to an "open" ion source greatly increases the complexity of relating ion source to ambient conditions. In addition to involved considerations of ion source geometry and angle of attack, a detailed knowledge of surface accommodation coefficients and reflection properties is necessary to arrive at a complete solution. In a survey of thermal accommodation coefficients, Hartnett[12] describes the difficulties in obtaining valid laboratory data. Consequently few data are available. In previous papers[13, 14] two limiting models were discussed. In one model it is assumed that perfect reflection occurs; i.e., the normal component of particle velocity is reversed upon collision with the surface. Assuming the surface to be an infinite plane (radius large compared to height of ion source above the surface)

$$n_a = n_g \Big/ \left[1 + \operatorname{erf} s\right] \tag{2}$$

where the velocity used to determine s is the component perpendicular to the plane surface. In the other model complete thermalization of the impinging particles is assumed prior to reemission. Then

$$n_a = 2n_g \Big/ \left[e^{-s^2}\sqrt{\frac{T_a}{T_s}} + \left(1 + s\sqrt{\pi\frac{T_a}{T_s}}\right)(1 + \operatorname{erf} s)\right] \tag{3}$$

where $T_s$ is the surface temperature.

The effect of these two models on the relative enrichment of $O_2$ over O is illustrated in Fig. 4 which is felt to represent the extreme cases. It should be noted that Fig. 4 is plotted only for positive values of V--the enrichment of O over $O_2$ for negative V can become virtually infinite 100 km below the peak of the trajectory since the instrument will be "outrunning" essentially all of the $O_2$.

The agreement between upleg and downleg $O/O_2$ ratios obtained by Schaefer and Nichols[13, 14] despite quite different angles of attack, suggests that the interaction during a single surface collision is closer to the perfect reflection model. Similar results obtained from three of the four more recent flights to be described tend to confirm this hypothesis.

In summary, the "open" ion source is capable of yielding more accurate ratios in the presence of highly reactive constitutents whereas measurements of stable constitutents within an orificed cavity are more

readily translated into ambient quantities. The ideal ion source would require either materials upon which surface recombination was negligible or a better knowledge of surface interaction processes.

3. Analyzers

The analysis of simple gases such as comprise the atmosphere requires only moderate resolution. Other factors such as compatability with an open ion source, weight, power and the measurement to be made dictate the choice of analyzer. Four types have been used in upper-atmosphere studies.

3.1 The Bennett radio-frequency mass spectrometer[15] was the first to successfully obtain upper-atmosphere composition data.[3, 16] Ions are accelerated to the same energy after which they pass a series of accurately spaced grids. Those ions having the correct velocity (and e/m ratio) to pass the grids in phase with the applied rf voltages abstract the maximum energy from the rf field. This serves as the basis to separate the ions of different e/m ratio. Due partly to the difficulties of employing an open ion source with this analyzer, it is no longer used in neutral mass spectrometry in this country.

3.2 The omegatron[17] creates ions in a crossed magnetic and rf electric field. The resonant ions describe an archimedes spiral and are then collected. Although incompatable with an open ion source, it has been used extensively in an orificed cavity to measure the concentrations of $N_2$.[18]

3.3 Magnetic mass spectrometers have been flown by Nier et al[8, 9] with an open ion source (Fig. 2) and, more recently, within an orificed cavity. They have yielded excellent results.[19, 20] This instrument accelerates the ions to a common energy into a transverse magnetic field. The radius of the ion path within the field is proportional to its momentum and the heavier particles describe curves of larger radii. One can now use the instrument as a momentum filter by employing a geometry which allows only one radius to reach the collector and then produce an analysis by sweeping the input energy and hence the mass of the particle having the required momentum. This principle was used by Nier. Another technique used by Spencer and Reber[10] is to place collectors along the radii corresponding to the gases one wishes to analyze and maintain the accelerating potential constant.

3.4 The massenfilter[21, 22] has been successfully flown many times by the University of Michigan. Ions are injected down the axis of a system of four rods spaced 90° apart (Fig. 5). When properly proportioned dc and rf voltages are applied to the rods, most of the ions become unstable under the action of the transverse fields. Unstable ions reach transverse amplitudes large enough to cause removal by collision with a rod. Only ions within a narrow range of e/m are stable and reach the collector. One of the chief advantages of this analyzer is its compatability with an open ion source.

This is due to the independence of indicated mass upon the injection energy. In an alternate mode of operation only rf voltages are applied to the rods. The output is now the sum of all ions of stable mass and lighter. As the rf voltage is swept, the output describes a staircase pattern. The chief advantage of this mode is that it serves as a calibration of the spectral peak heights and it also shows the sum of all ion currents due to masses beyond the range of the instrument.

4. Recent Results

In this calendar year two massenfilter Nike-Apache rockets were launched from Fort Churchill, Canada and four from the Mobile Launch Expedition, two near the equator and two near $60^{o}$ south latitude. Of these the day-night pair at Fort Churchill and the nighttime equatorial shot were completely successful. A malfunction in the daytime equatorial shot prevented actuation of the filament but spectra at very much lower sensitivity were obtained nevertheless because the exposed grid accelerated ambient electrons through the ionizing volume.

Because of time limitations, the major effort has been concentrated on a comparison of the data between Fort Churchill and two earlier Wallops Island Nike-Apache massenfilter firings. Firing information is available in Table 1 and a summary of the more significant comparisons appears in Table 2.

To provide a feeling for the quality of the data, Fig. 6 is a reproduction of a typical telemetered set of spectra and Fig. 7 is a selected plot of raw data points to illustrate typical scatter and consistency between upleg and downleg points. The remaining figures are the curves from which the related comparison summaries of Table II were obtained. For simplicity, individual data points were omitted.

In comparing curves, only the data of the two Fort Churchill flights, NASA 14.11 and 14.95UA, are unambiguously diurnal. The eight months separating the Wallops Island flights have undoubtedly introduced seasonal and solar cycle effects in the data. Likewise, the time differences between the Wallops Island firings and the Fort Churchill firings introduce similar effects in those comparisons. However, it is assumed the major effects are diurnal and geographic and the comparisons of Figs. 8 to 18 are so captioned. In support of this assumption, the daytime $N_2$ densities observed at Wallops Island are approximately twice as large as the nighttime in common with the observations of Spencer, et al.[18] Further, the $O/O_2$ daytime ratios are larger than the nighttime in qualitative agreement with Hall, Schweizer and Hinteregger.[23] Despite large and random seasonal differences in the dates of acquisition of these various sets of data, density and composition changes appear to correlate chiefly with time of day.

4.1 $O/O_2$ comparisons. A nominal accelerating grid potential of 47 volts was used in the Wallops Island flights. As described elsewhere,[13, 14] the ionization cross-sections for O and $O_2$ are essentially equal under these conditions, and the number density ratios are equal to the ion current ratios. For greater sensitivity, the Fort Churchill flights used a 65 volt grid and, by a similar process, it was determined the ionization

cross-section of $O_2$ was 5-10% greater than O in these payloads. Hence the Fort Churchill $O/O_2$ current ratios have been multiplied by 1.07 to yield the number density ratios shown in Figs. 8 through 11.

Figs. 8 and 9 clearly show greater $O/O_2$ ratios during the daytime flights at both locations. For purposes of comparison, data published by Nier, et al[9] have been plotted on Fig. 8. Figs. 10 and 11 show the ratios to be larger at Wallops Island than at Fort Churchill. Throughout, the greater ratios are coincident with larger values of solar EUV flux which causes the dissociation.

4.2 $A/N_2$ separation ratio. Of interest in determining the altitude region characterized by turbulent mixing and that controlled by diffusive equilibrium is the $A/N_2$ separation ratio defined as the $A/N_2$ number density (or current) ratio obtained at altitude divided by the number density (or current) ratio obtained from a sample of ground air. Figs. 12 and 13 compare day-night data for both locations. Both sets of curves tend to indicate a higher level of turbulent mixing in the daytime although the effect at Fort Churchill is not very great. This may be due to atmospheric motions associated with the diurnal bulge and the stronger effects at Wallops Island due to its closer proximity to the sub-solar point. Similar data obtained from Fig. 1 of Hedin and Nier[20] and Table 4 of Hedin, Avery, and Tschetter[19] are plotted on Fig. 12 for comparison. Figs. 14 and 15 make latitude comparisons of the separation ratio. They indicate the slope of the ratio is greater at Wallops Island than at Fort Churchill, consistent with higher temperatures over Fort Churchill.

Whether the inflections in the curve for the Fort Churchill nighttime firing and in that derived from the data of Hedin and Nier and of Hedin,

Avery and Tschetter are real is speculative. Fig. 16, the separation ratio obtained from a much earlier daytime flight at Wallops Island,[13, 14] is included for comparison and supports the validity of the inflections in the curves.

4.3 $O_2/N_2$ ratios. Only two comparisons, Figs. 17 and 18 of the $O_2/N_2$ ratios are shown. These ratios generally decrease with altitude but the daytime values show the steeper gradient. Intercomparison of Figs. 17 and 18 shows that the Fort Churchill ratios are always the higher. Throughout, the ratios are lower when there is a greater solar EUV input to the atmosphere which results in loss of $O_2$ due to dissociation.

## 5. Conclusion

Until a better understanding is gained of the effects which occur at a surface in a very few collisions, it would appear no single instrument can yield accurate data on both ambient number densities and the ratios involving unstable constituents. As a solution to the conflicting instrumentation specifications, two separate instruments, one with an open ion source and one in a cavity, have the possibility of a complete determination by intercorrelation of the data. A step in this direction has already been taken by the group at the University of Minnesota under the direction of A. O. Nier.

Several diurnal and geographic trends have been noted in recent experiments. However, these are not completely devoid of possible seasonal and/or solar cycle effects. Further day-night flights and flights performed essentially simultaneously at widely separated latitudes will be required to remove the ambiguities.

Acknowledgments

The work described herein has been supported by the National Aeronautics and Space Administration. Special thanks are due J. Brown and J. Briggs for the reduction of the data and preparation of the figures.

TABLE I

Nike-Apache Launch Data

| NASA No. | Place | Date | Local Time | Peak Altitude (km) |
|---|---|---|---|---|
| 1408 | Wallops Island | 28 Mar 63 | 0255 | 190 |
| 1410 | Wallops Island | 26 Nov 63 | 1316 | 172 |
| 1411 | Ft. Churchill | 18 Feb 65 | 1409 | 195 (est.) |
| 1495 | Ft. Churchill | 19 Feb 65 | 0317 | 187 |

TABLE II

Comparison Summaries

| | Day | Night |
|---|---|---|
| $n(O)/n(O_2)$ | | |
| Wallops Island | 9 at 180 km (extrapolated)<br>1 at 117 km | 5.8 at 180 km<br>1 at 118 km |
| Ft. Churchill | 6 at 180 km<br>1 at 128 km | 4.6 at 180 km<br>1 at 127 km |
| $O_2/N_2$ Current Ratio | | |
| Wallops Island | 0.1 at 123 km<br>0.054 at 170 km | 0.1 at 121 km<br>0.075-0.08 at 145-180 km |
| Ft. Churchill | 0.1 at 147 km<br>0.075 at 180 km | 0.1 at 155 km<br>0.095 at 185 km |
| $A/N_2$ Separation Ratios | | |
| Wallops Island | 1 at 106 km<br>0.26 at 130 km | 1 at 99 km<br>0.36 at 125 km |
| Ft. Churchill | 1 at 95 km (extrapolated)<br>0.25 at 150 km | 1 at 100 km (extrapolated)<br>0.28 at 150 km |

## REFERENCES


1. D. S. Hacker, S. A. Marshall, and M. Steinberg. Recombination of Atomic Oxygen on Surfaces. J. Chem. Phys. 35 (1961), 1788-1792.

2. J. Wood and H. Wise. The Interaction of Atoms with Solid Surfaces, Rarefied Gas Dynamics. Academic Press, New York (1961), 51-59.

3. E. B. Meadows and J. W. Townsend. IGY Rocket Measurements of Arctic Atmospheric Composition Above 100 km. Space Research I (1960). Ed. H. K. Kallmann-Bijl, North-Holland, Amsterdam, 175-198.

4. A. A. Pokhunkov. The Study of Upper Atmosphere Neutral Composition at Altitudes Above 100 km. Space Research I (1960), Ed. H. K. Kallmann-Bijl, North-Holland Publishing Co., 101-106.

5. A. A. Pokhunkov. Mass-Spectrometer Investigations of the Structural Parameters of the Earth's Atmosphere at Altitudes from 100 to 210 km. Planetary Space Sci. 9 (1962), 269-279.

6. A. A. Pokhunkov. Gravitational Separation, Composition and Structural Parameters of the Night Atmosphere at Altitudes between 100 and 210 km. Planetary Space Sci. 11 (1963), 441-449.

7. A. A. Pokhunkov. On the Variation in the Mean Molecular Weight of Air in the Night Atmosphere at Altitudes of 100 to 200 km from Mass Spectrometer Measurements. Planetary Space Sci. 11 (1963), 297-304.

8. A. O. Nier, J. H. Hoffman, C. Y. Johnson, and J. C. Holmes. Neutral Composition of the Atmosphere in the 100 to 200 Kilometer Range. Journal of Geophysical Research 69 (1964), 979-989.

9. A. O. Nier, J. H. Hoffman, C. Y. Johnson, and J. C. Holmes. Neutral Constituents of the Upper Atmosphere: The Minor Peaks Observed in a Mass Spectrometer. Journal of Geophysical Research 69 (1964), 4629-4636.

10. N. W. Spencer and C. A. Reber. A Mass Spectrometer for an Aeronomy Satellite. Space Research III (1962), 1151-1155.

11. R. Horowitz, and H. E. LaGow, Upper Air Pressure and Density Measurements from 90 to 220 Kilometers with the Viking 7 Rocket. Journal of Geophysical Research 62 (1957), 57-78.

12. J. P. Hartnett. A Survey of Thermal Accommodation Coefficients. Rarefied Gas Dynamics. Ed. L. Talbot. (1961), 1-28.

13. E. J. Schaefer and M. H. Nichols. Neutral Composition Obtained from a Rocket-Borne Mass Spectrometer. Space Research IV (1964), 205-234.

14. E. J Schaefer and M. H. Nichols. Upper Air Neutral Composition Measurements by a Mass Spectrometer. Journal of Geophysical Research 69 (1964), 4649-4660.

15. Willard H. Bennett. Radiofrequency Mass Spectrometer. Journal of Applied Physics 21 (1950), 143-149.

16. Edith Meadows-Reed and Charles R. Smith. Mass Spectrometric Investigations of the Atmosphere between 100 and 227 Kilometers above Wallops Island, Virginia. Journal of Geophysical Research 69 (1964), 3199-3212.

17. H. Sommer, H. A. Thomas and J. A. Hipple. The Measurement of e/M by Cyclotron Resonance. Phys. Rev. 82 (1951), 697-702.

18. N. W. Spencer and L. H. Brace, G. R. Carignan, D. R. Taeusch, and H. Niemann. Electron and Molecular Nitrogen Temperature and Density in the Thermosphere. Journal of Geophysical Research 70 (1965), 2665-2698.

19. A. E. Hedin, C. P. Avery, and C. D. Tschetter. An Analysis of Spin Modulation Effects on Data Obtained with a Rocket-Borne Mass Spectrometer. Journal of Geophysical Research 69 (1964), 4637-4648.

20. A. E. Hedin and Alfred O. Nier. Diffusive Separation in the Upper Atmosphere. Journal of Geophysical Research 70 (1965), 1273-1274.

21. W. Paul, H. P. Reinhard, and U. Von Zahn. Das Elektrische Massenfilter als Massenspektrometer und Isotopentrenner. Zeitschrift fur Physik 152 (1958), 143-182.

22. E. J. Schaefer and M. H. Nichols. Mass Spectrometer for Upper Air Measurements. Am. Rocket Soc. J. 31 (1961), 1773-1776.

23. L. H. Hall, W. Schweizer, and H. E. Hinteregger. Diurnal Variation of the Atmosphere around 190 Kilometers Derived from Solar Extreme Ultraviolet Absorption Measurements. Journal of Geophysical Research 68 (1963), 6413-6417.

# LIST OF FIGURES


1. University of Michigan ion source.
2. University of Minnesota arrangement of ion sources.
3. Southwest Center for Advanced Study ion source.
4. Relative enrichment of $O_2$ over O.
5. Laboratory massenfilter showing analyzer rods.
6. Telemetered Spectrums. Shown, from the top down, are the time code, the monitor channel which shows the sweep voltage, the high gain channel, the medium gain channel, and the low gain channel. Peak type spectrums alternate with the staircase type. Calibrations appear on the left.
7. Raw data points.
8. Diurnal Comparison of $n(O)/n(O_2)$ at Wallops Island. Despite an 8-months difference in firings, the major variant is assumed to be diurnal. See text.
9. Diurnal Comparison of $n(O)/n(O_2)$ at Fort Churchill.
10. Latitude comparison of $n(O)/n(O_2)$ - Daytime.
11. Latitude comparison of $n(O)/n(O_2)$ - Nighttime.
12. Diurnal Comparison of $Ar\text{-}N_2$ Separation Ratio at Wallops Island.
13. Diurnal Comparison of $Ar\text{-}N_2$ Separation Ratio at Fort Churchill.
14. Latitude Comparison of $Ar\text{-}N_2$ Separation Ratio - Daytime.
15. Latitude Comparison of $Ar\text{-}N_2$ Separation Ratio - Nighttime.
16. $Ar\text{-}N_2$ Separation Ratio, Nike-Cajun NASA 10.91 UA.
17. Diurnal Comparison of $O_2/N_2$ Current Ratio at Wallops Island.
18. Diurnal Comparison of $O_2/N_2$ Current Ratio at Fort Churchill.

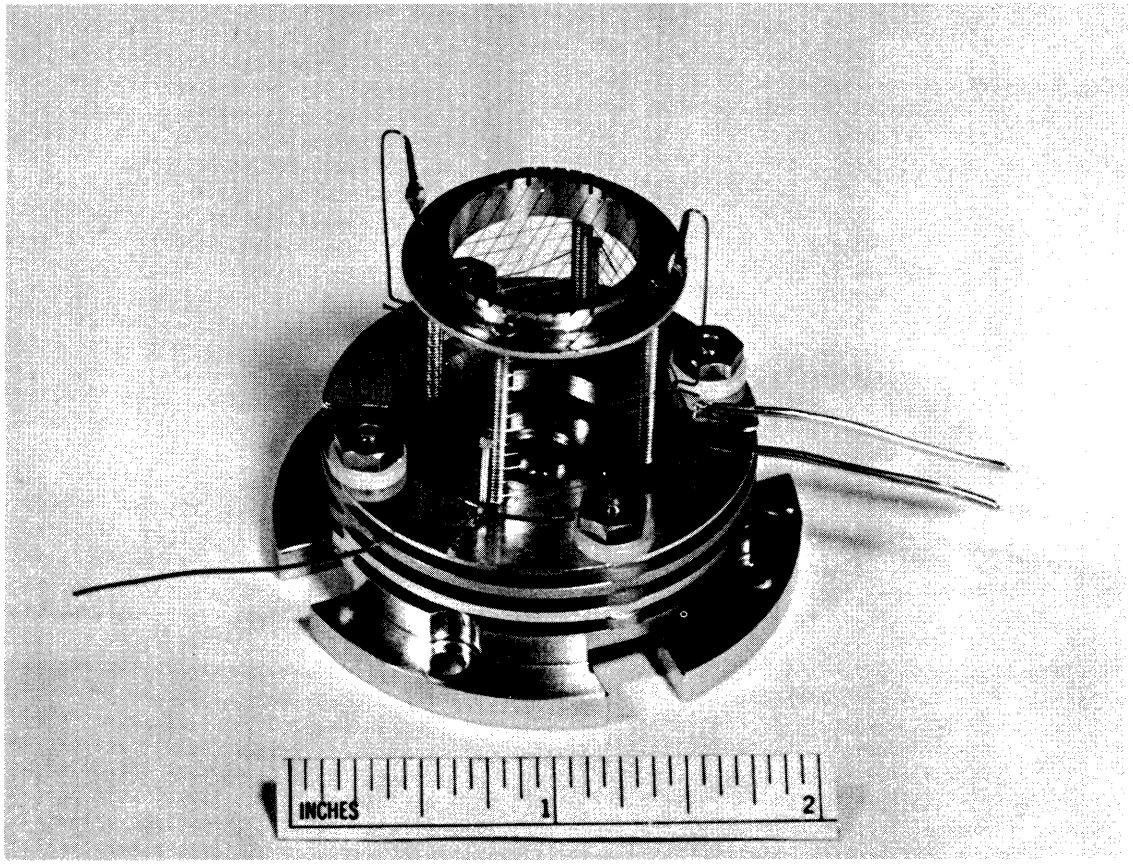


Fig. 1

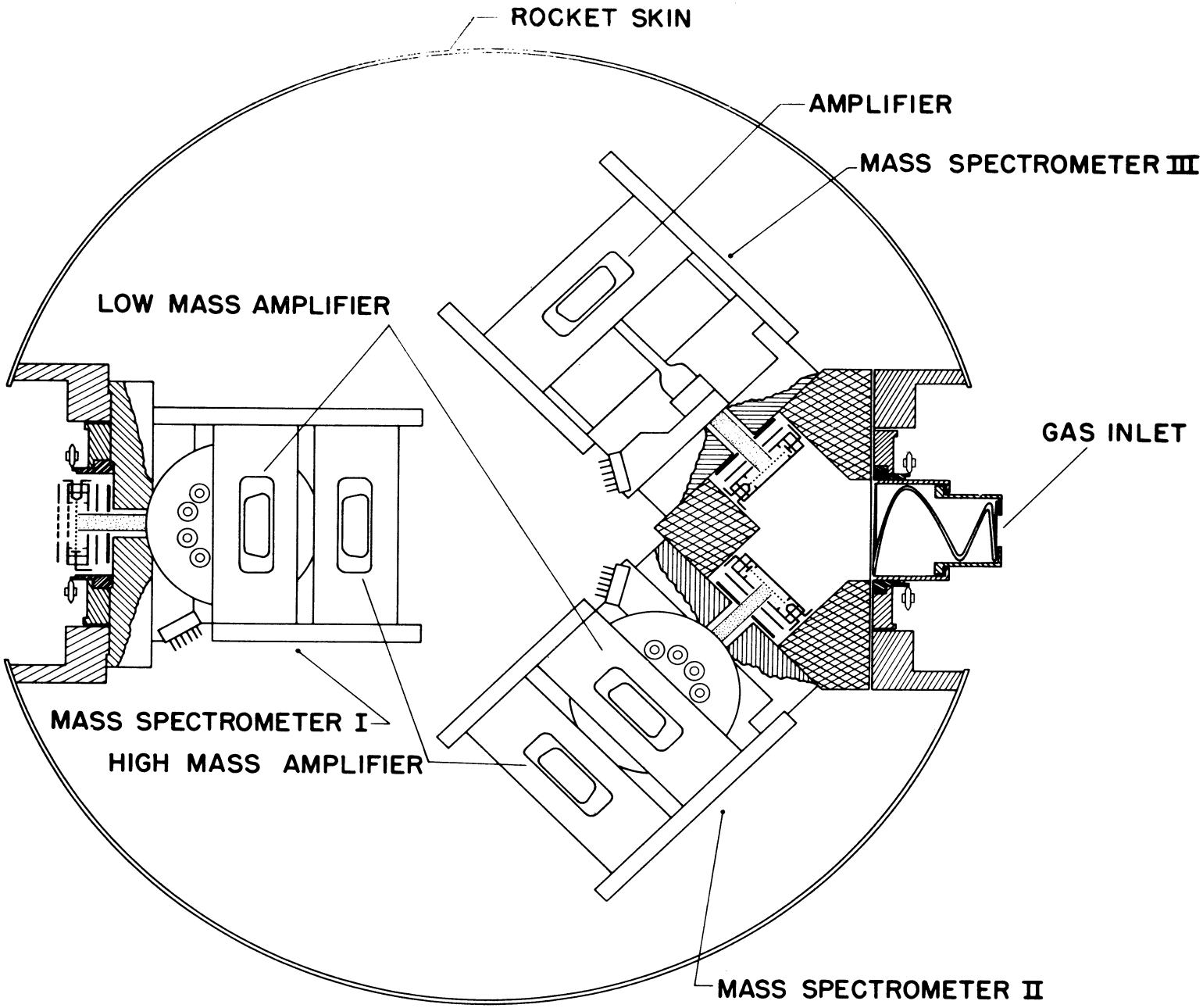
ROCKET SKIN
AMPLIFIER
MASS SPECTROMETER III
LOW MASS AMPLIFIER
GAS INLET
MASS SPECTROMETER I
HIGH MASS AMPLIFIER
MASS SPECTROMETER II

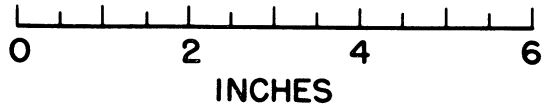
0
2
4
6
INCHES

Fig. 2

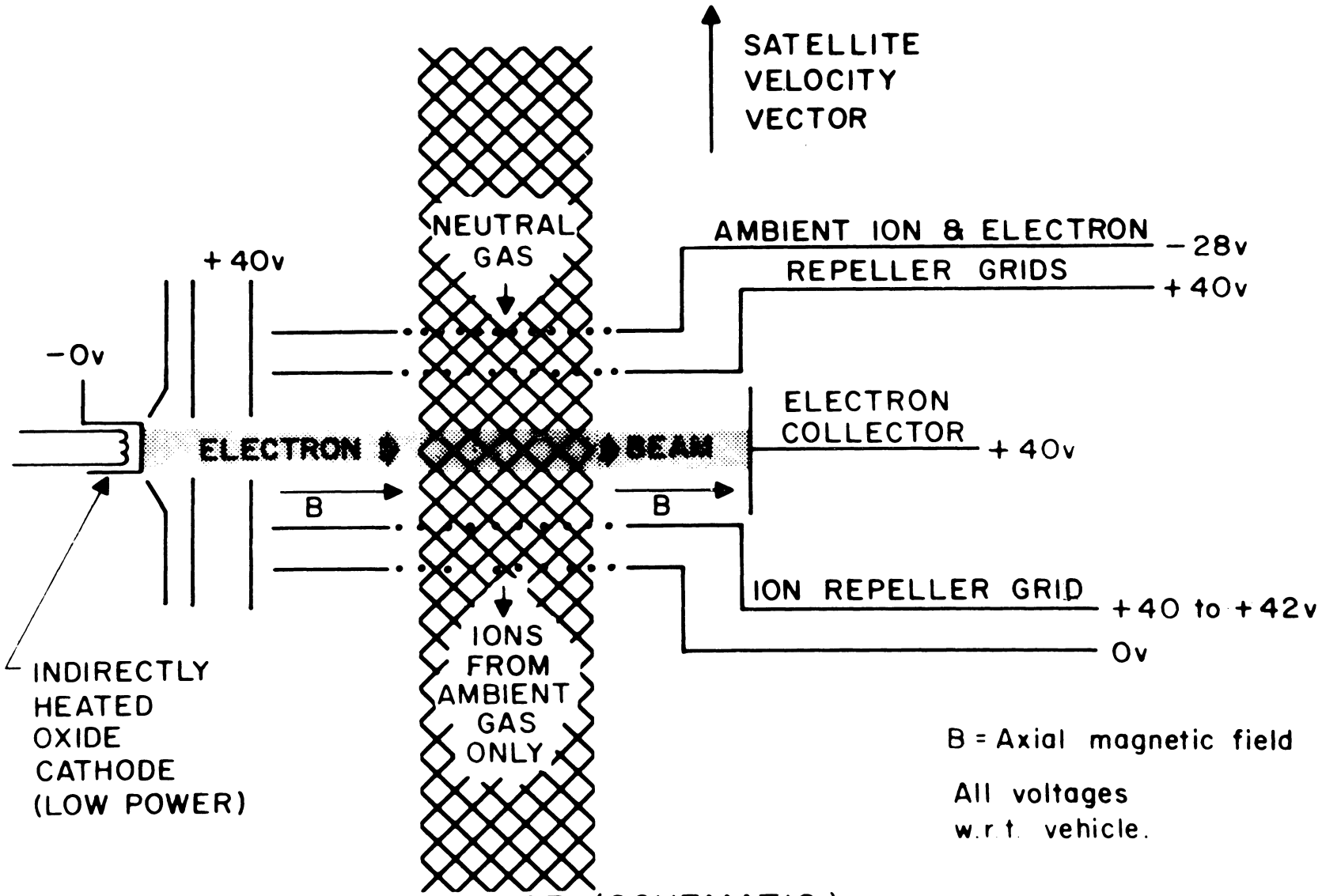


ION SOURCE (SCHEMATIC)

utilizing an orientated satellite's own motion to discriminate between ambient atmospheric gases and contaminate gases.

Fig. 3

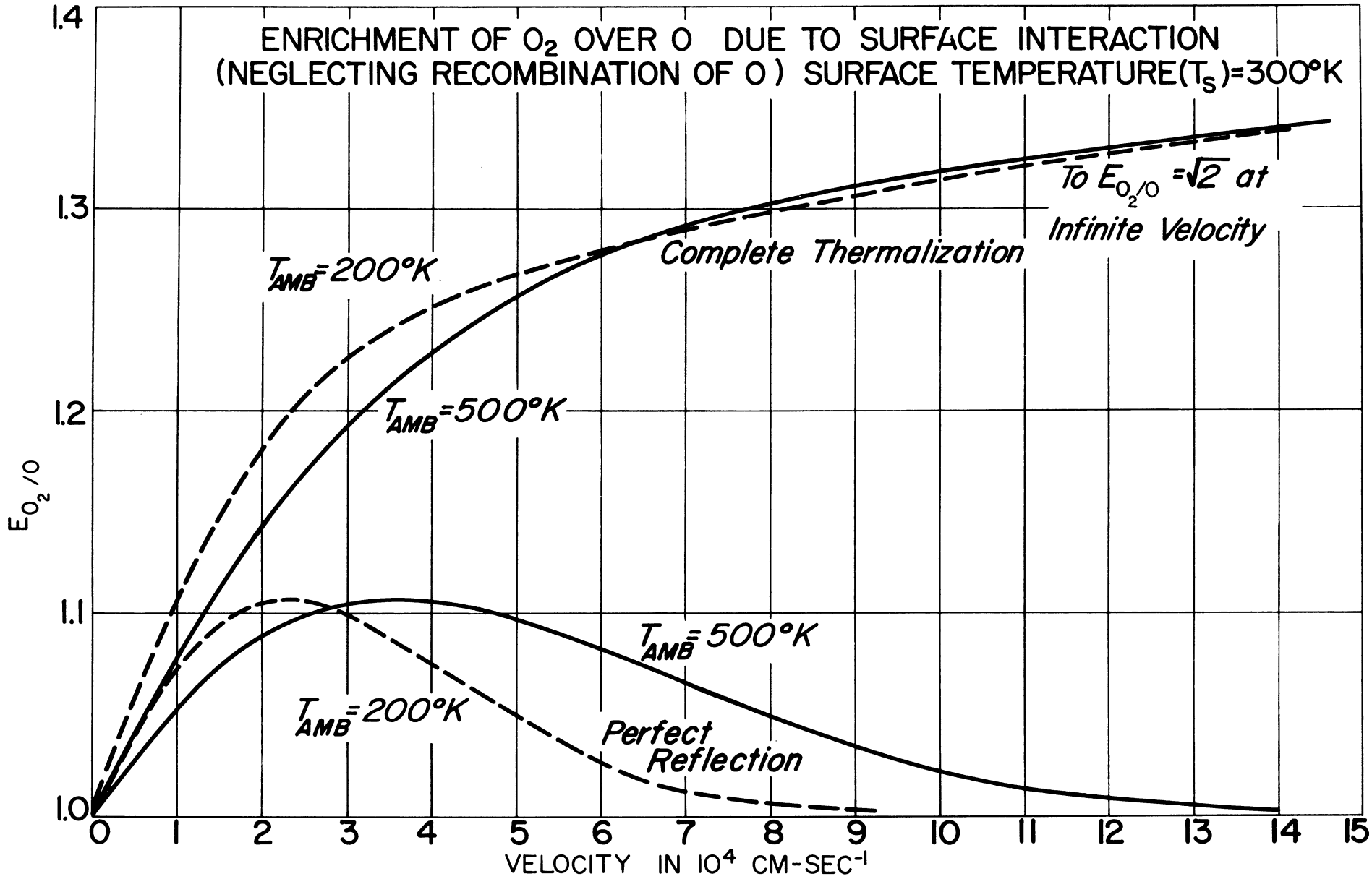
ENRICHMENT OF $O_2$ OVER O DUE TO SURFACE INTERACTION
(NEGLECTING RECOMBINATION OF O) SURFACE TEMPERATURE($T_S$)=300°K
To $E_{O_2/O}$ =√2 at Infinite Velocity
Complete Thermalization
$T_{AMB}$=200°K
$T_{AMB}$=500°K
$T_{AMB}$=500°K
$T_{AMB}$=200°K
Perfect Reflection
$E_{O_2/O}$
1.4
1.3
1.2
1.1
1.0
0 1 2 3 4 5 6 7 8 9 10 11 12 13 14 15
VELOCITY IN $10^4$ CM-SEC$^{-1}$

Fig. 4

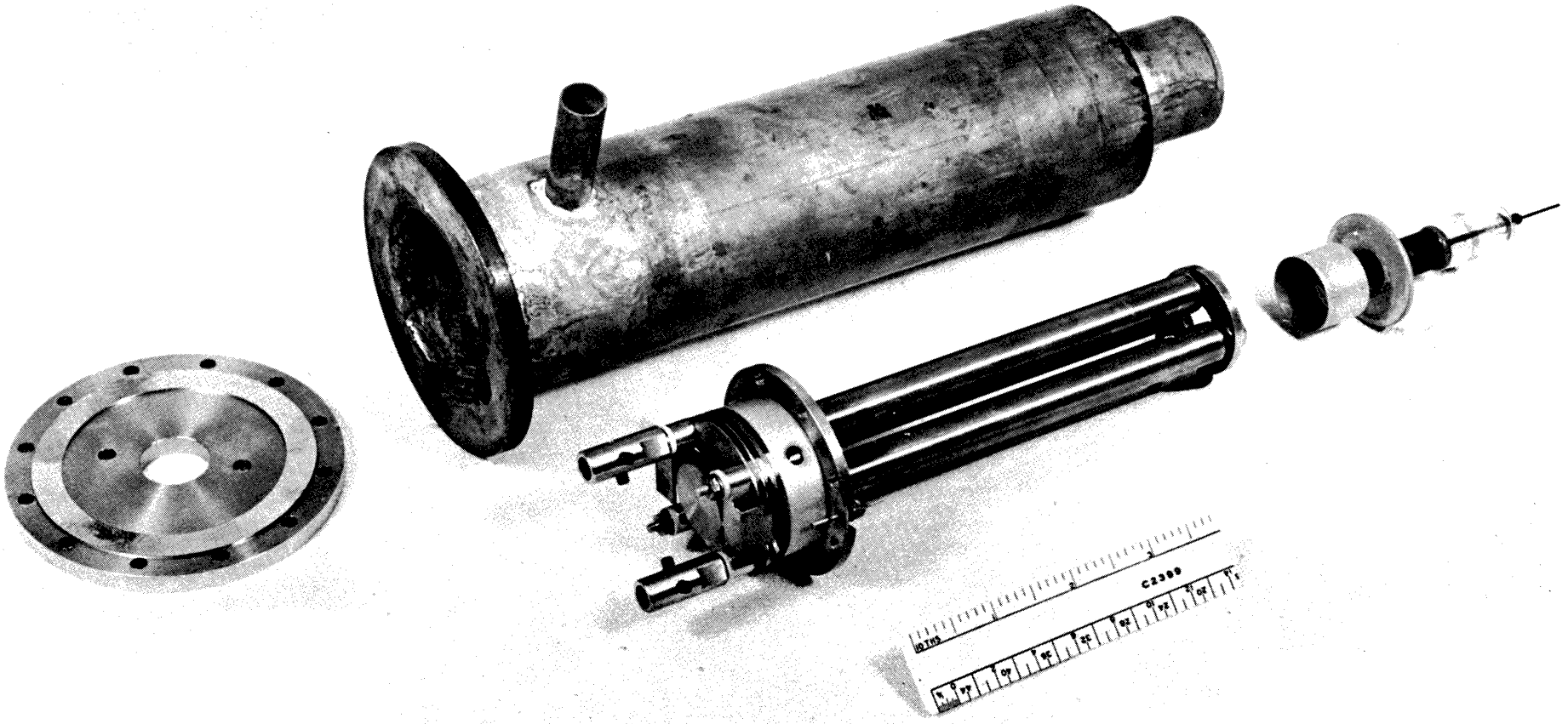

Fig. 5

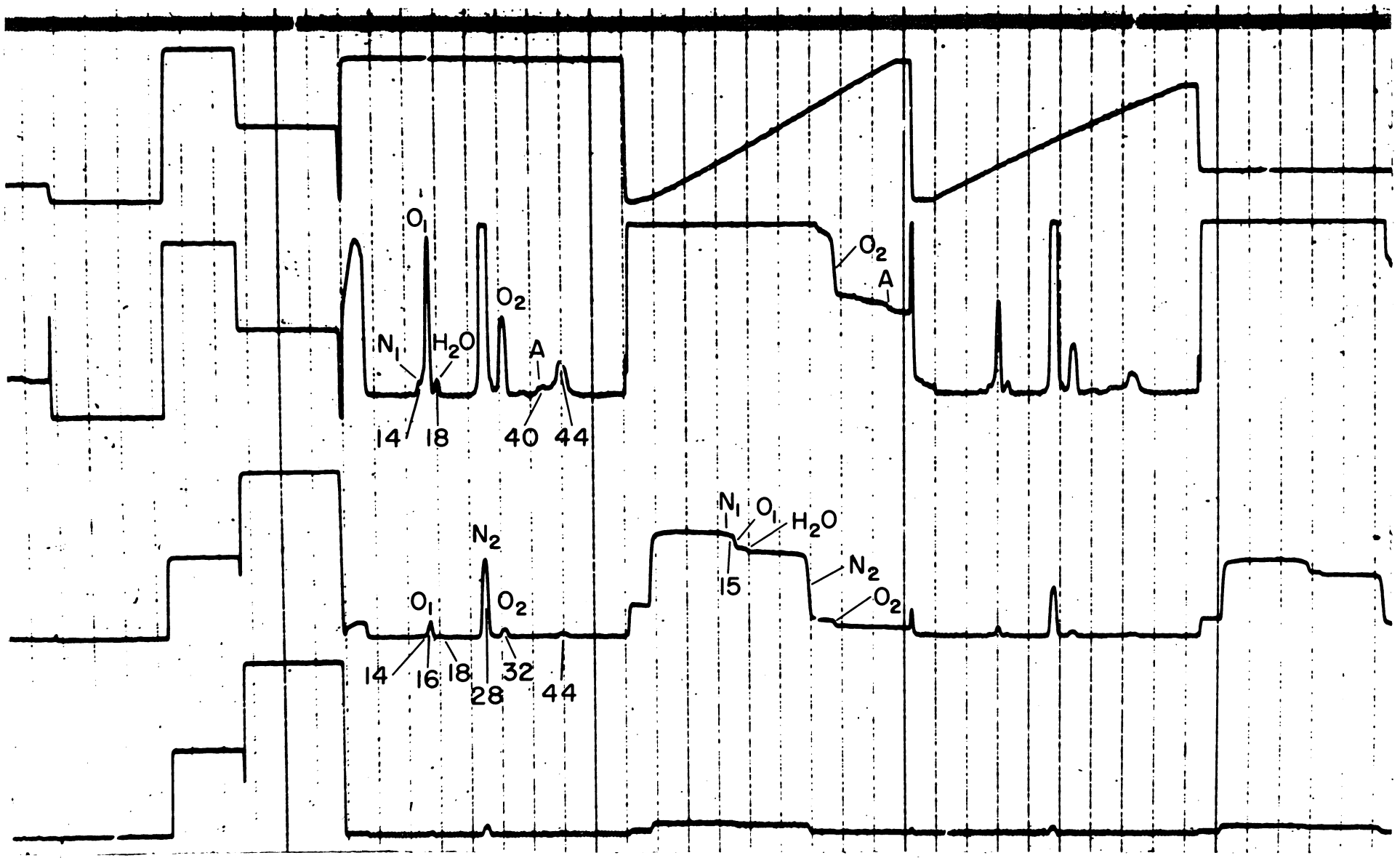


NIKE-APACHE-1408 UA---131KM-UPLEG-107SEC

Fig. 6

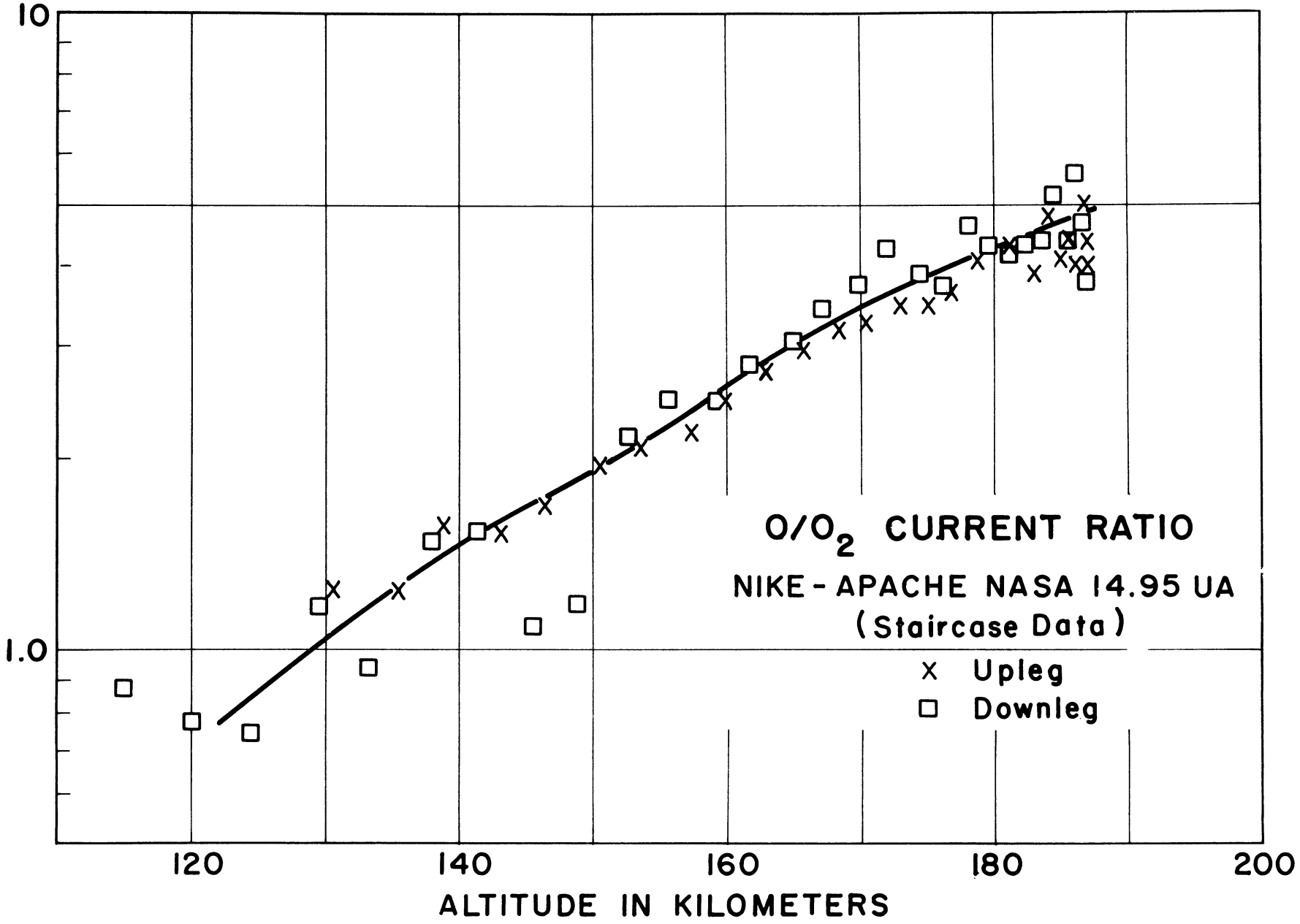
10
1.0
120
140
160
180
200
ALTITUDE IN KILOMETERS
O/O2 CURRENT RATIO
NIKE - APACHE NASA 14.95 UA
(Staircase Data)
X Upleg
□ Downleg

Fig. 7

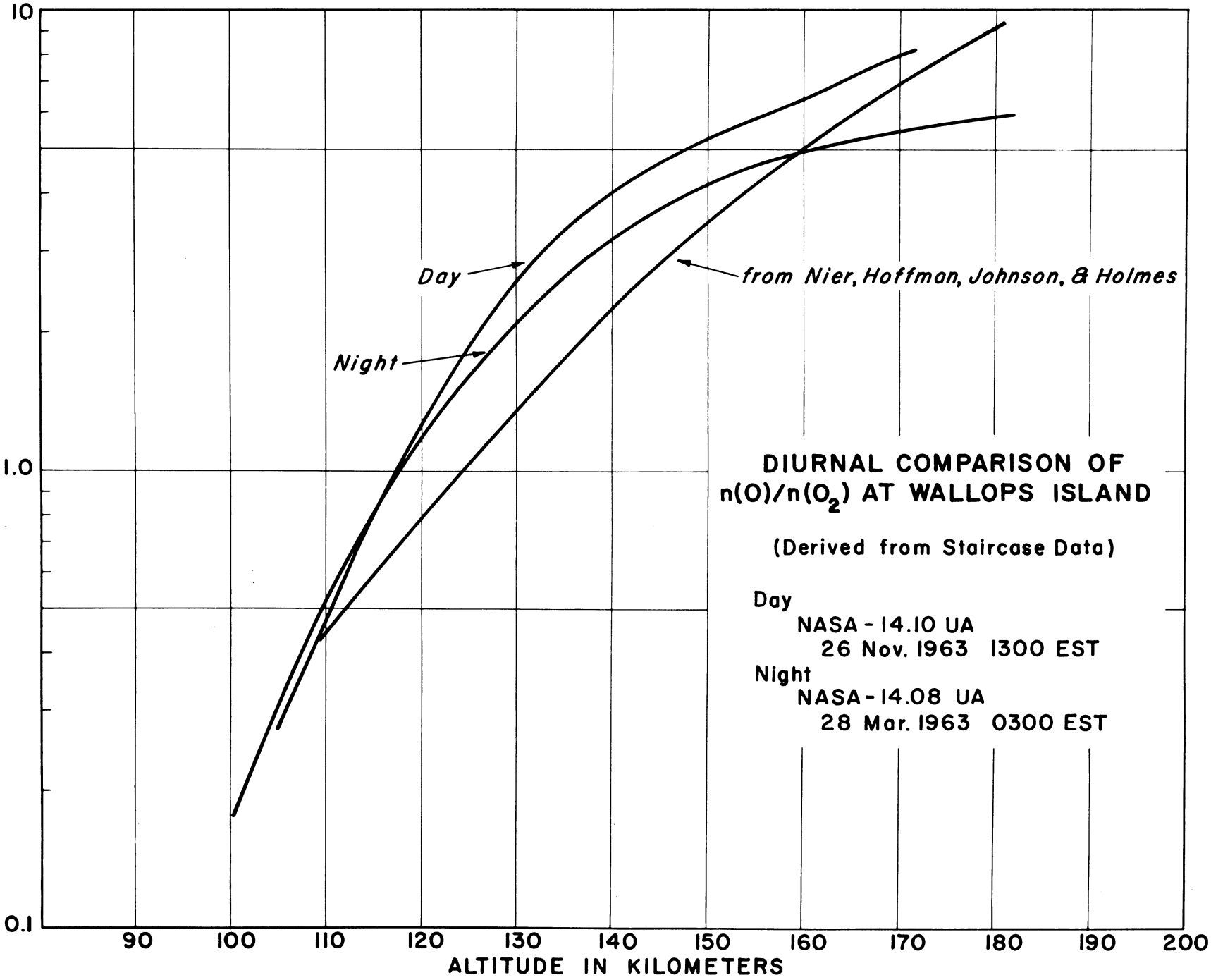
10
1.0
0.1
90
100
110
120
130
140
150
160
170
180
190
200
ALTITUDE IN KILOMETERS
Day
Night
from Nier, Hoffman, Johnson, & Holmes
DIURNAL COMPARISON OF
n(O)/n(O2) AT WALLOPS ISLAND
(Derived from Staircase Data)
Day
NASA - 14.10 UA
26 Nov. 1963 1300 EST
Night
NASA - 14.08 UA
28 Mar. 1963 0300 EST

Fig. 8

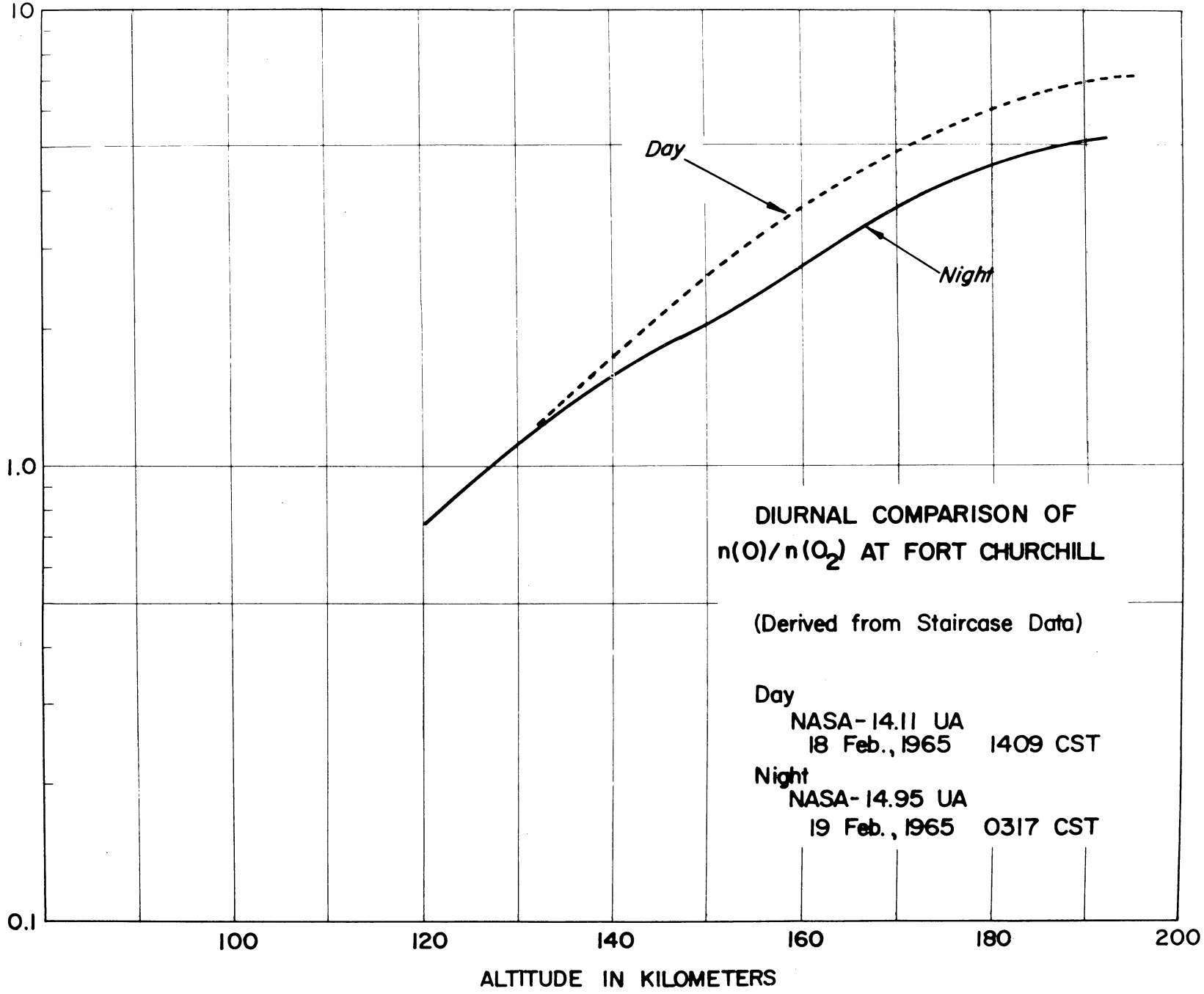
10
1.0
0.1
Day
Night
DIURNAL COMPARISON OF
n(O)/n(O2) AT FORT CHURCHILL
(Derived from Staircase Data)
Day
NASA-14.11 UA
18 Feb., 1965 1409 CST
Night
NASA-14.95 UA
19 Feb., 1965 0317 CST
100
120
140
160
180
200
ALTITUDE IN KILOMETERS

Fig. 9

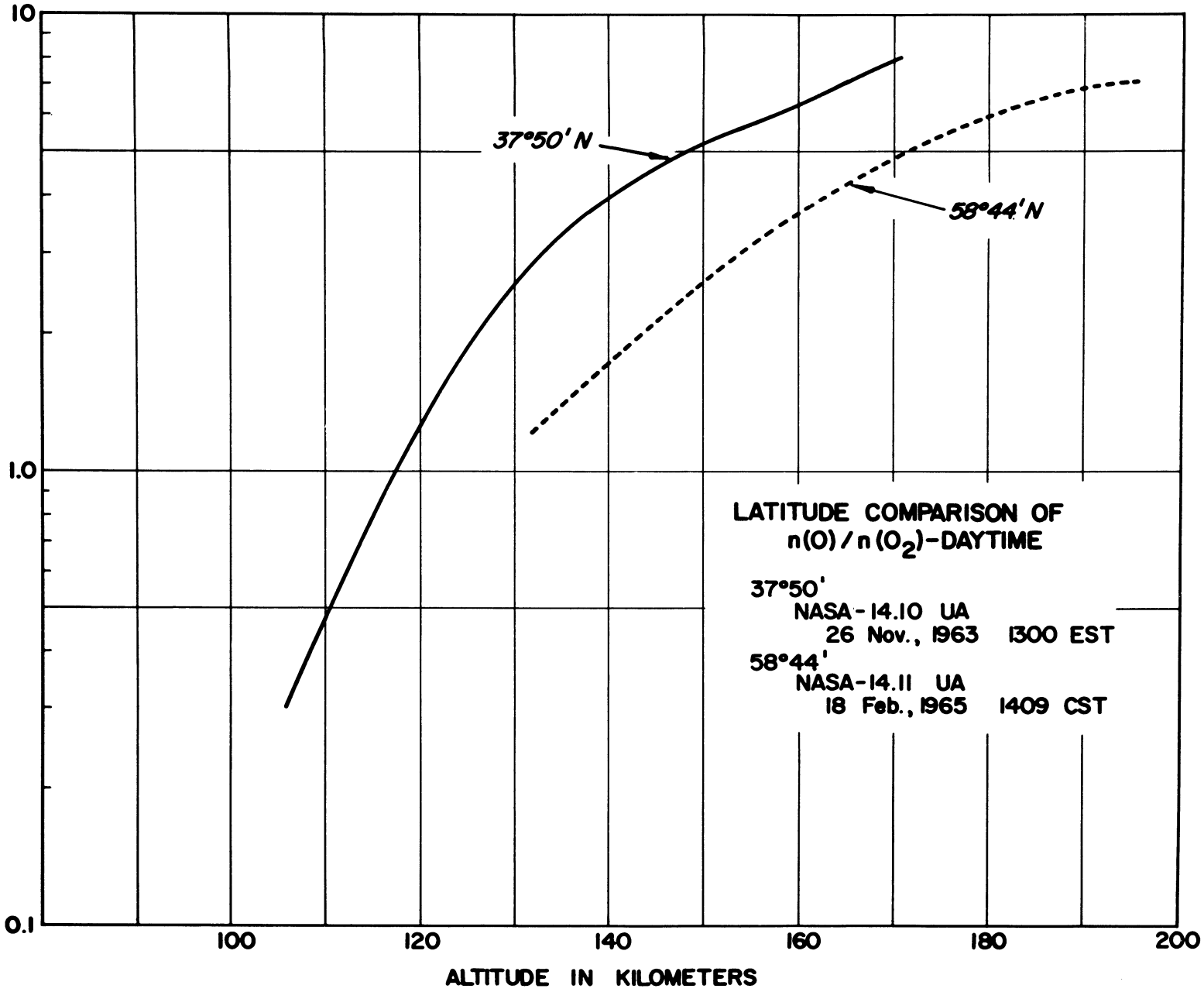
10
1.0
0.1
37°50' N
58°44' N
LATITUDE COMPARISON OF
n(O) / n(O2)-DAYTIME
37°50'
NASA-14.10 UA
26 Nov., 1963 1300 EST
58°44'
NASA-14.11 UA
18 Feb., 1965 1409 CST
100
120
140
160
180
200
ALTITUDE IN KILOMETERS

Fig. 10

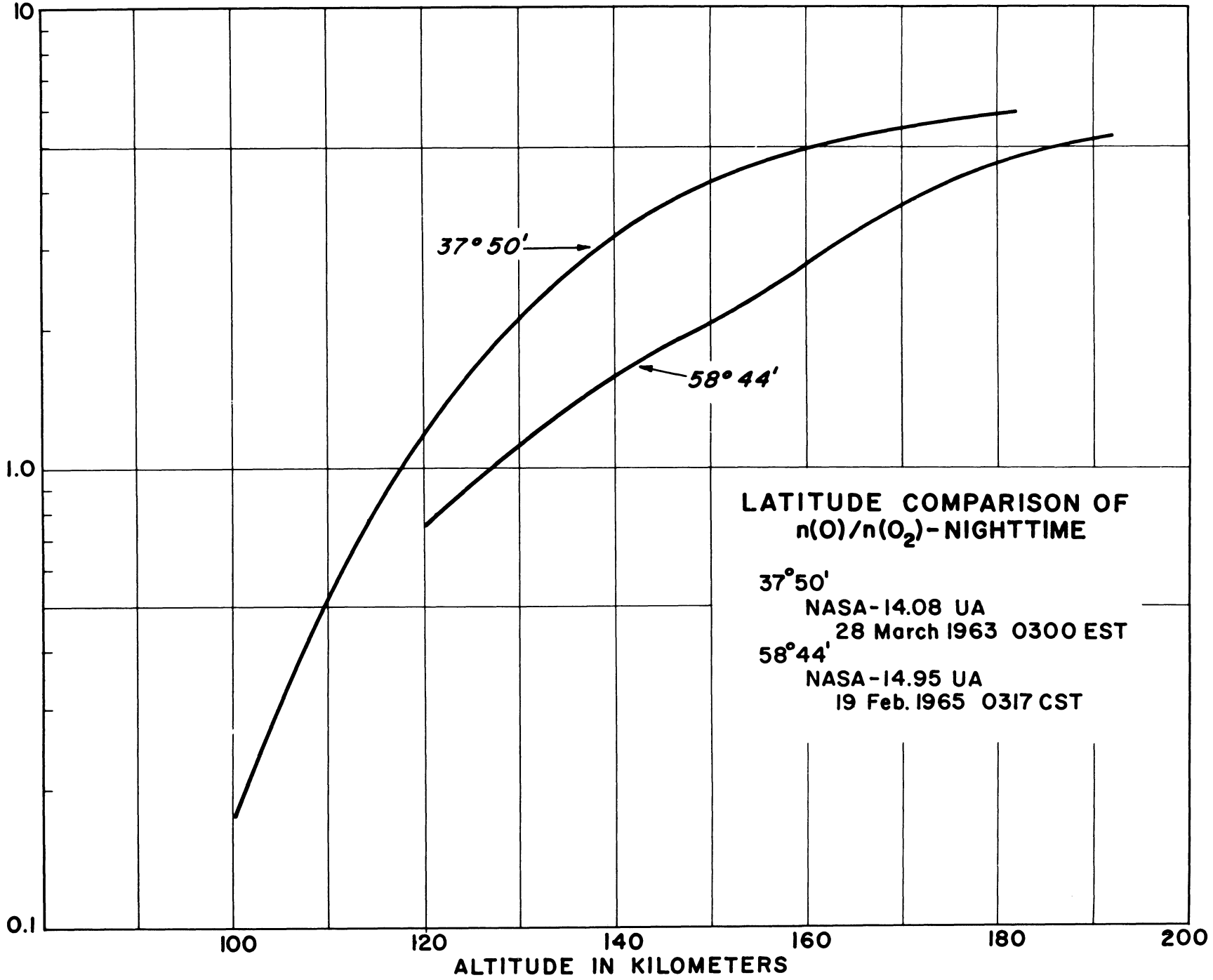
10
1.0
0.1
37° 50'
58° 44'
LATITUDE COMPARISON OF
n(O)/n(O2) - NIGHTTIME
37°50'
NASA-14.08 UA
28 March 1963 0300 EST
58°44'
NASA-14.95 UA
19 Feb. 1965 0317 CST
100
120
140
160
180
200
ALTITUDE IN KILOMETERS

Fig. 11

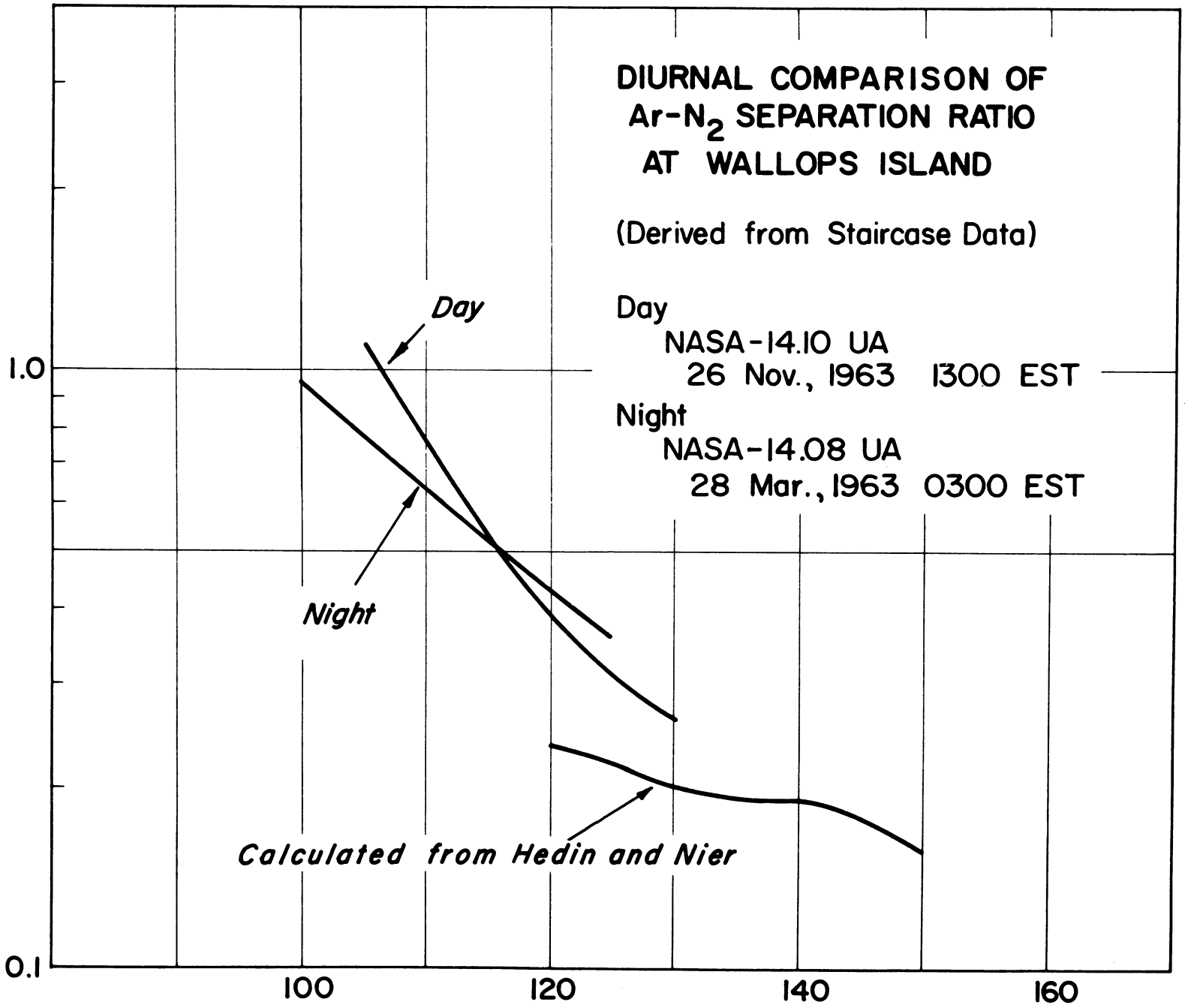
DIURNAL COMPARISON OF
Ar-N2 SEPARATION RATIO
AT WALLOPS ISLAND
(Derived from Staircase Data)
Day
NASA-14.10 UA
26 Nov., 1963 1300 EST
Night
NASA-14.08 UA
28 Mar., 1963 0300 EST
Day
Night
Calculated from Hedin and Nier
1.0
0.1
100
120
140
160
ALTITUDE IN KILOMETERS

Fig. 12

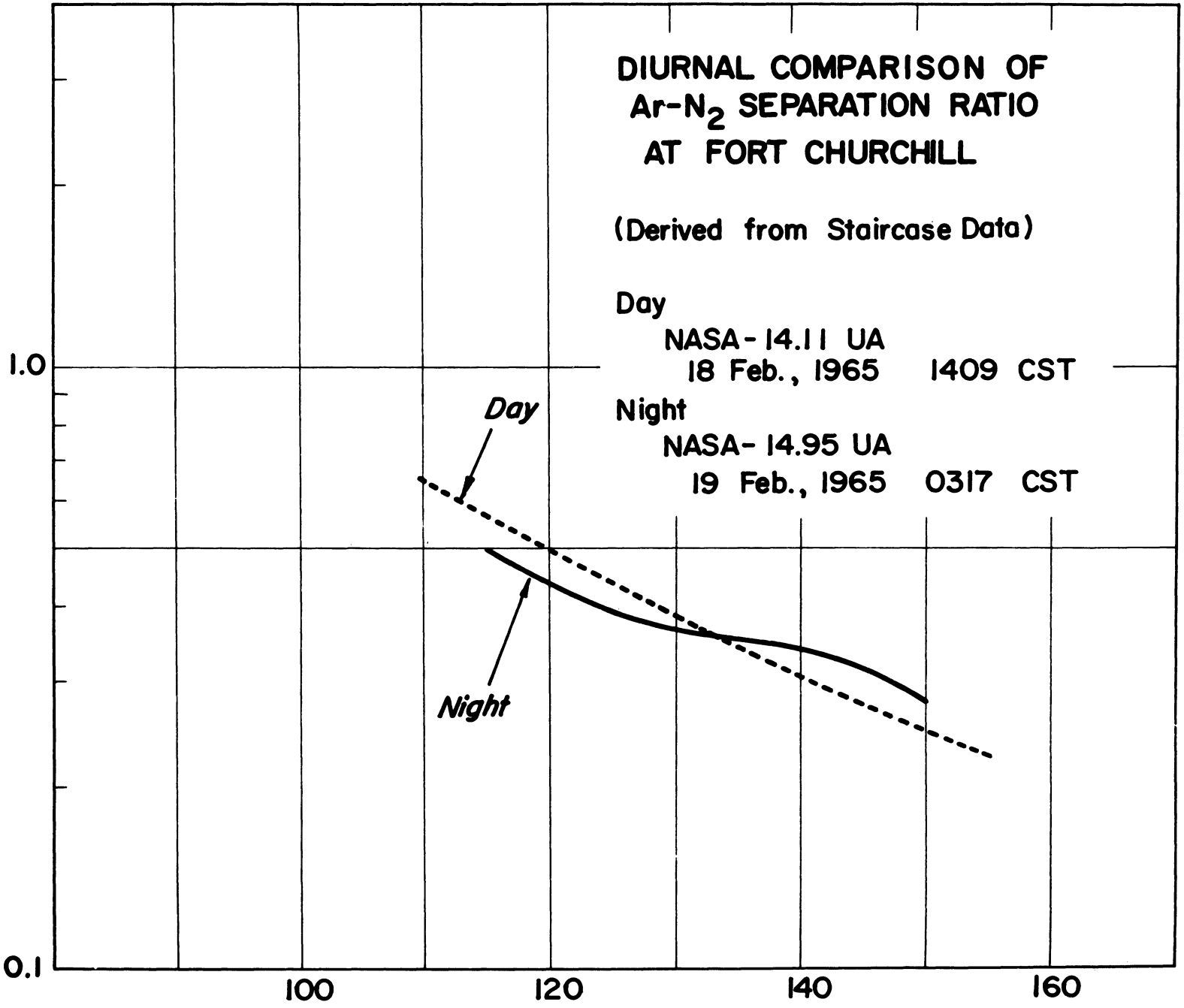
DIURNAL COMPARISON OF
Ar-N2 SEPARATION RATIO
AT FORT CHURCHILL
(Derived from Staircase Data)
Day
NASA-14.11 UA
18 Feb., 1965 1409 CST
Night
NASA-14.95 UA
19 Feb., 1965 0317 CST
Day
Night
1.0
0.1
100
120
140
160
ALTITUDE IN KILOMETERS

Fig. 13

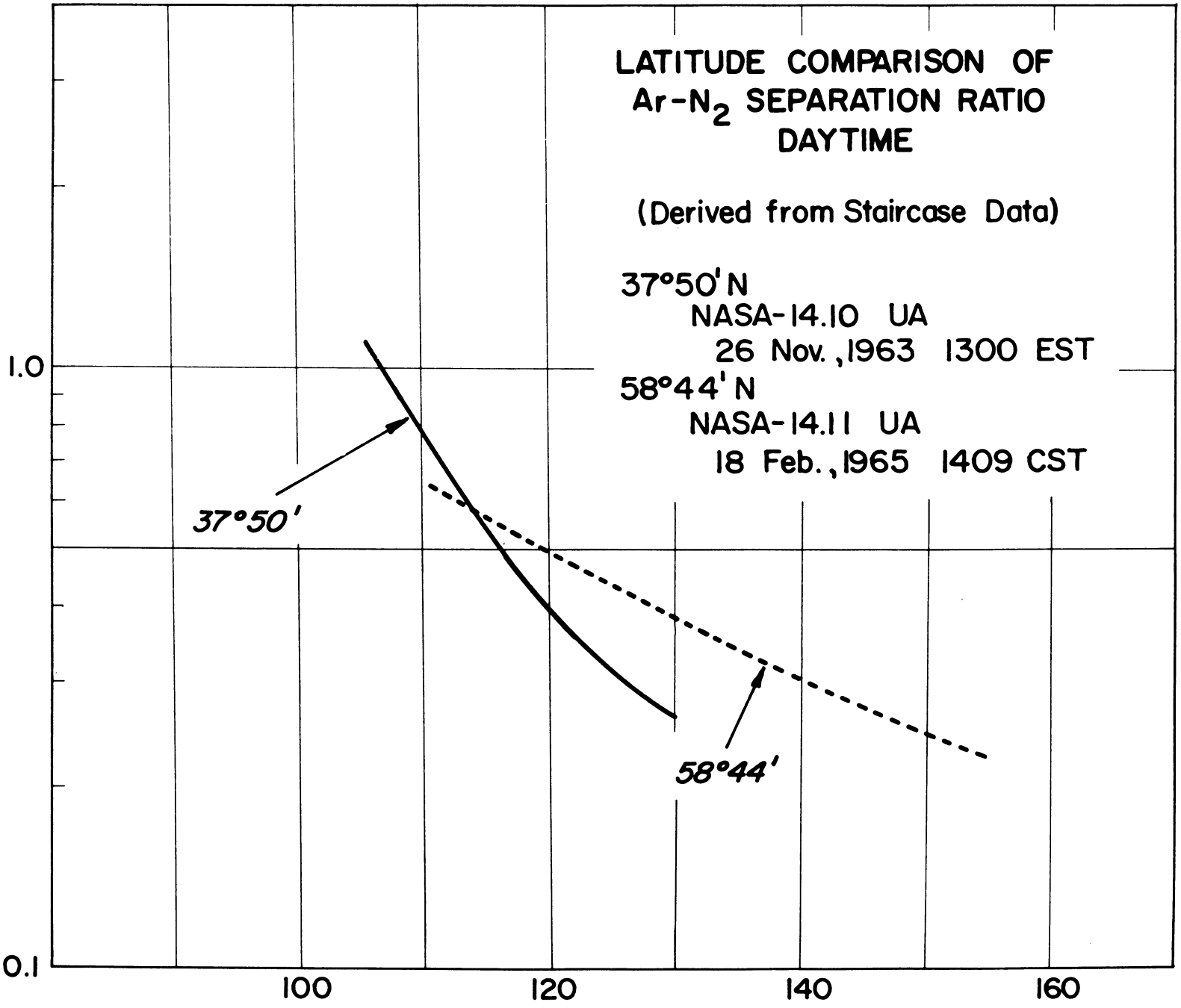
LATITUDE COMPARISON OF
Ar-N2 SEPARATION RATIO
DAYTIME
(Derived from Staircase Data)
37°50' N
NASA-14.10 UA
26 Nov., 1963 1300 EST
58°44' N
NASA-14.11 UA
18 Feb., 1965 1409 CST
37°50'
58°44'
1.0
0.1
100
120
140
160
ALTITUDE IN KILOMETERS

Fig. 14

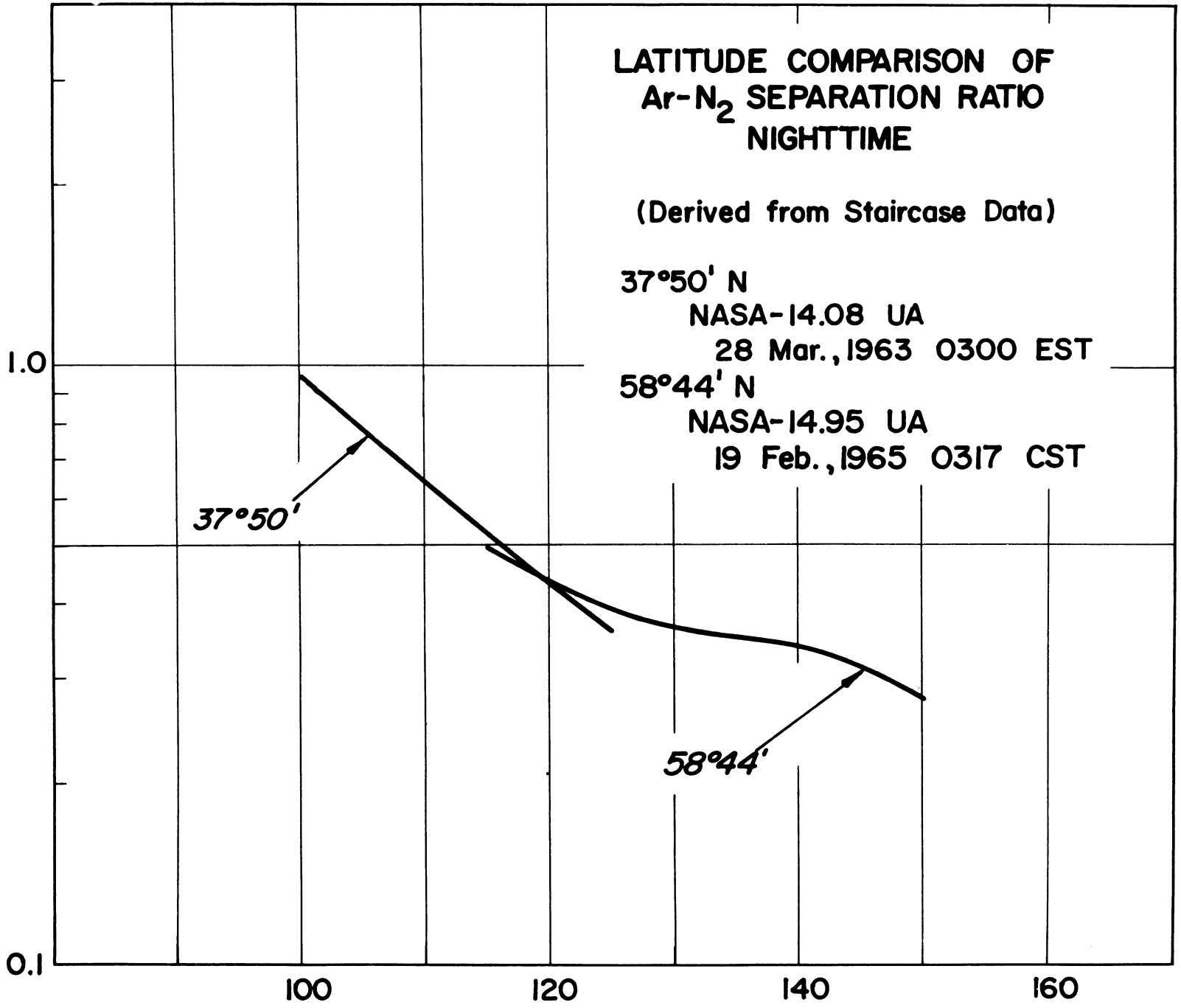
LATITUDE COMPARISON OF
Ar-N2 SEPARATION RATIO
NIGHTTIME
(Derived from Staircase Data)
37°50' N
NASA-14.08 UA
28 Mar., 1963 0300 EST
58°44' N
NASA-14.95 UA
19 Feb., 1965 0317 CST
37°50'
58°44'
1.0
0.1
100
120
140
160
ALTITUDE IN KILOMETERS

Fig. 15

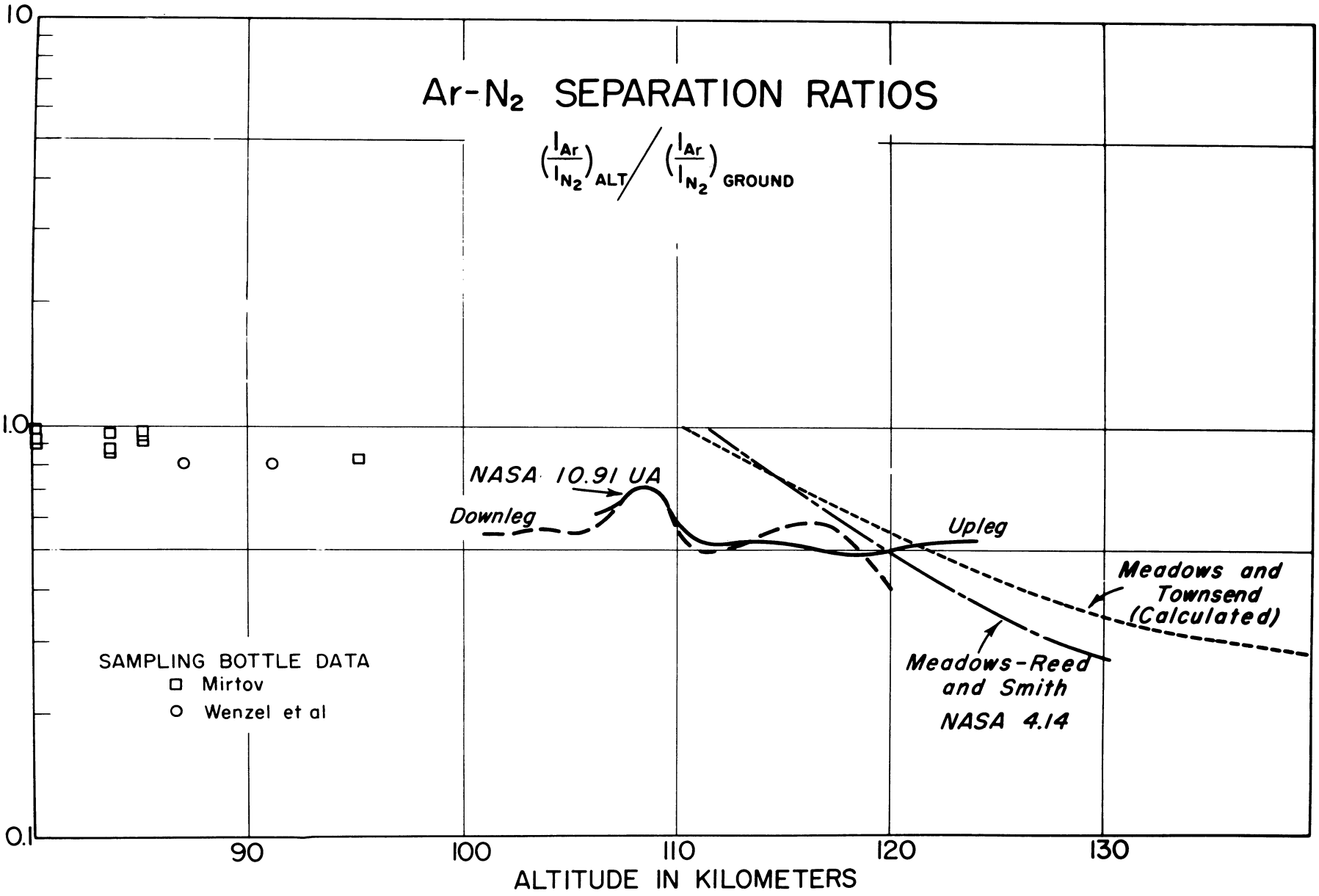
Ar-N2 SEPARATION RATIOS
(IAr/IN2)ALT / (IAr/IN2)GROUND
10
1.0
0.1
NASA 10.91 UA
Downleg
Upleg
Meadows and Townsend (Calculated)
Meadows-Reed and Smith NASA 4.14
SAMPLING BOTTLE DATA
Mirtov
Wenzel et al
90
100
110
120
130
ALTITUDE IN KILOMETERS

Fig. 16

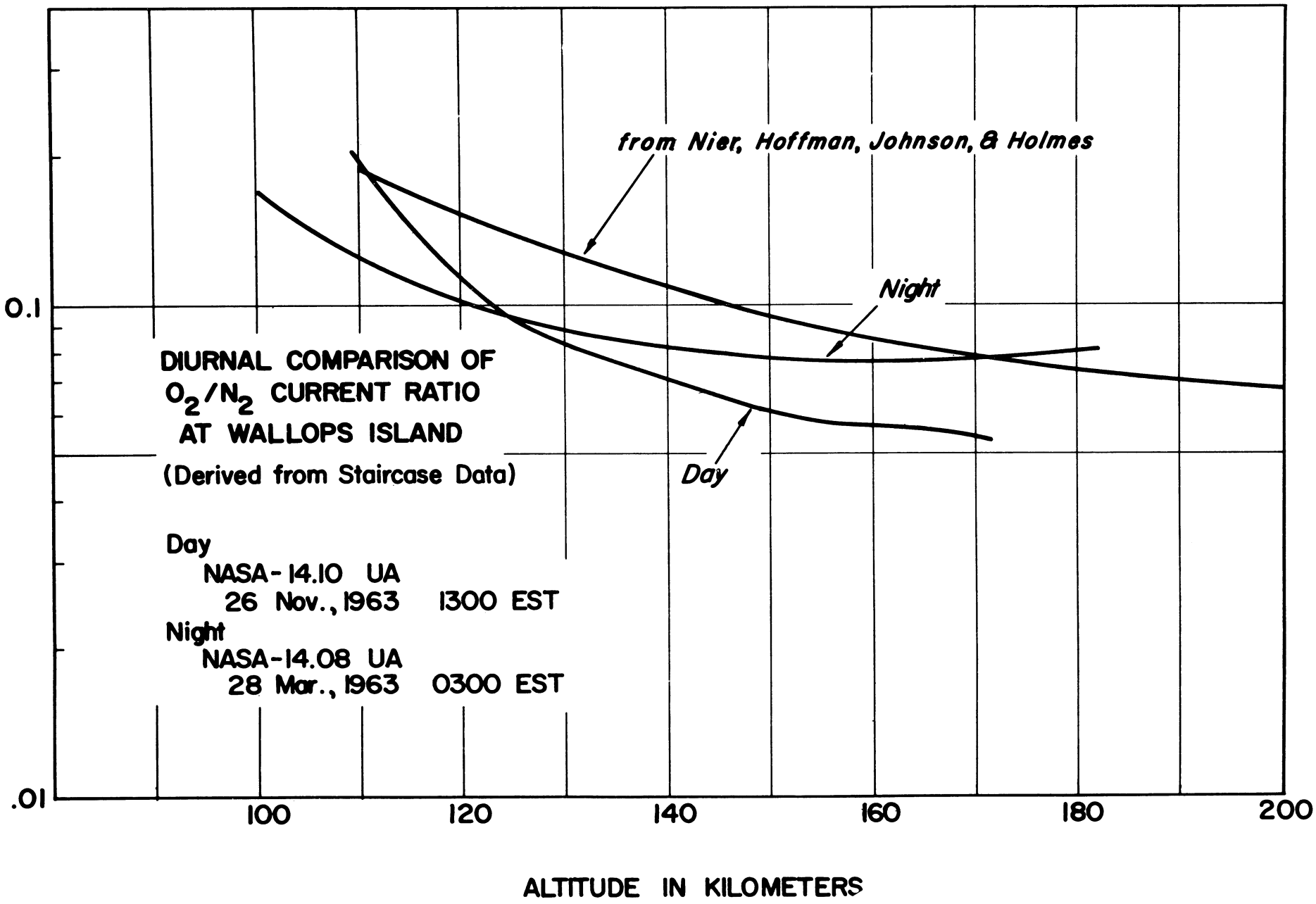
from Nier, Hoffman, Johnson, & Holmes
Night
Day
DIURNAL COMPARISON OF
$O_2/N_2$ CURRENT RATIO
AT WALLOPS ISLAND
(Derived from Staircase Data)
Day
NASA-14.10 UA
26 Nov., 1963 1300 EST
Night
NASA-14.08 UA
28 Mar., 1963 0300 EST
0.1
.01
100
120
140
160
180
200
ALTITUDE IN KILOMETERS

Fig. 17

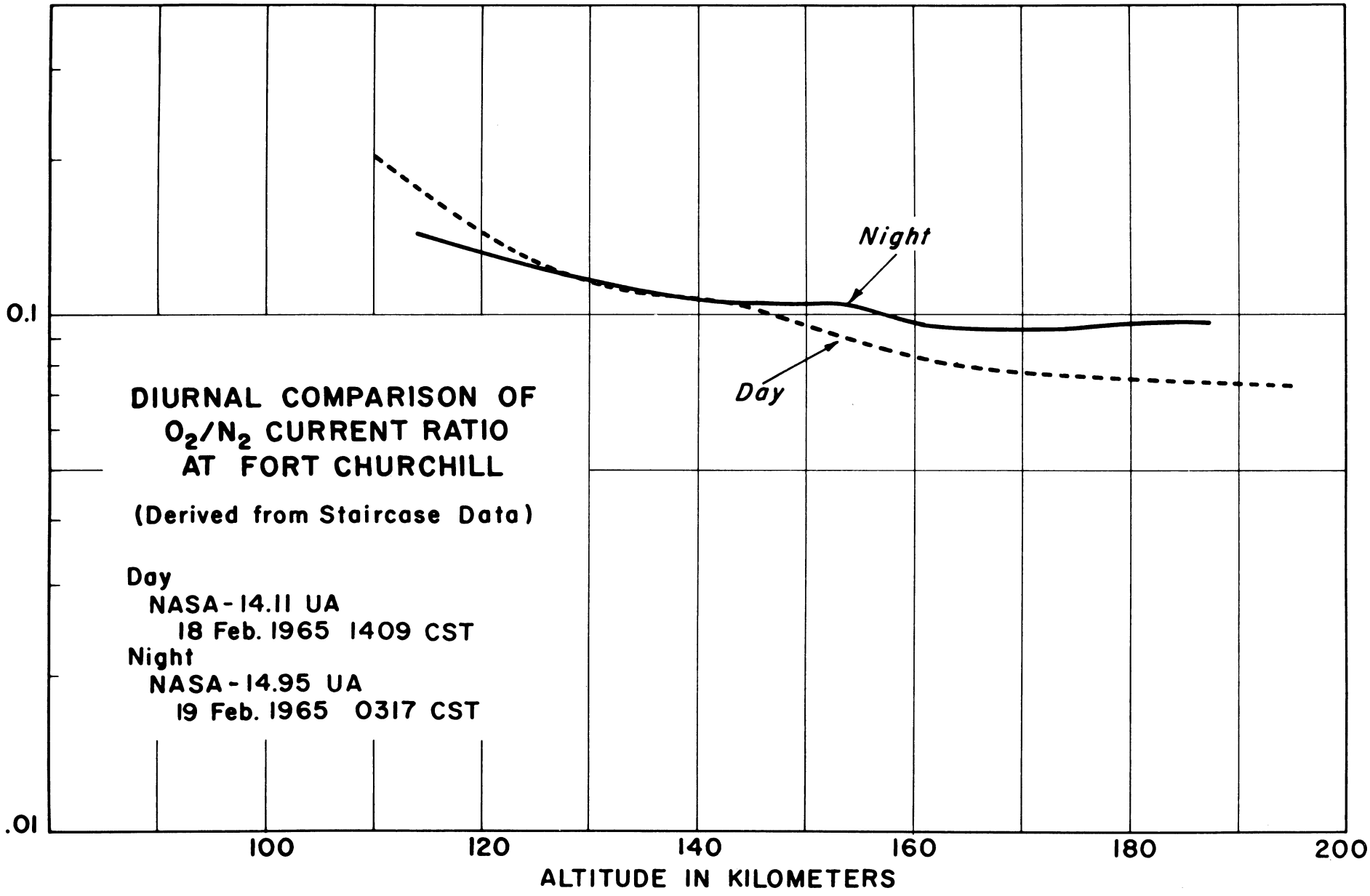
0.1
.01
Night
Day
DIURNAL COMPARISON OF
$O_2/N_2$ CURRENT RATIO
AT FORT CHURCHILL
(Derived from Staircase Data)
Day
NASA-14.11 UA
18 Feb. 1965 1409 CST
Night
NASA-14.95 UA
19 Feb. 1965 0317 CST
100
120
140
160
180
200
ALTITUDE IN KILOMETERS

Fig. 18